Applied Energy 305 (2022) 117677

Contents lists available at ScienceDirect

Applied Energy

journal homepage: www.elsevier.com/locate/apenergy

Performance and dynamics of active greywater heat recovery in buildings

Bruno Hadengue [a,b,*], Eberhard Morgenroth [a,b], Tove A. Larsen [a], Luca Baldini [c,d]

[a] Eawag, Swiss Federal Institute of Aquatic Science and Technology, 8600 Dübendorf, Switzerland
[b] ETH Zürich, Institute of Environmental Engineering, 8093 Zürich, Switzerland
[c] ZHAW, Zurich University of Applied Sciences, 8401 Winterthur, Switzerland
[d] Empa, Swiss Federal Institute for Materials Science and Technology, 8600 Dübendorf, Switzerland

HIGHLIGHTS

- We investigate active greywater heat recovery with heat pumps under various conditions.
- Colder climates and large hot water consumption induce larger electricity savings.
- We identify and compare various system configurations for heat recovery.
- Closed-loop systems, with greywater as direct heat source, show largest potential.

ARTICLE INFO

Keywords:
Greywater heat recovery
Decentralized
Heat pump
Domestic hot water
Wastewater
Energy efficiency

ABSTRACT

In the effort to de-carbonize the building stock, heat pumps are increasingly utilized in Switzerland, with 70% of the fast-growing heat pump market using ambient air as heat source. Inexpensive and easy to implement, these heat pumps are, however, less efficient than their ground- or water-source counterparts. In this modeling study, we aim at increasing the efficiency of air-source heat pumps using domestic greywater-contained heat. We assess the performance improvement relative to standard heat pump configurations across various climates, seasons, building envelopes, and domestic hot water consumption patterns. The results show that the annually-averaged coefficient of performance improves by 4.1% on average – ranging from 0.6% to 7.5%. This efficiency gain translates on average to 1.8 kWh/week of compressor electricity savings. Although attractive due to its simplicity, the proposed open-loop configuration – preheating of an external heat source – only leads to moderate performance improvement of air-source heat pumps. Based on these results, we extensively discuss and compare alternative system configurations and identify several fundamental differences in the heat recovery dynamics of each configuration. We show that closed-loop systems – using greywater as direct heat source – show the largest performance improvement potential, although being more expensive and complex to implement.

1. Introduction

The residential sector commonly accounts for 30 – 40% of the final energy consumption – and carbon dioxide emissions – in OECD countries [1]. In their effort to mitigate global warming, the European Union (EU) and Switzerland aim at reducing the carbon footprint of their building stock: in the EU, the Energy Performance of Buildings Directive (EPBD) requires that all new buildings must be nearly zero energy buildings from 2021 [2]. In Switzerland, the 2050 Energy Strategy aims at a 45 % reduction in residential primary energy use compared to 2010 [3].

In line with the push for building efficiency, heat generation for space heating (SH) and domestic hot water (DHW) use is undergoing a massive shift from oil furnaces to electric heat pumps. In Switzerland, electric heat pumps cover more than 18 % of the total heated floor area, compared to 10 % in 2011 [4]. About 70 % of these systems use ambient air as a heat source [5]. Inexpensive and easy to implement, air-source heat pumps are, however, less efficient than their water- or ground-source counterparts, with typical seasonal performance factors of roughly 3.5 vs. 4.5 [6]. This is accentuated by the low heat pump efficiency in winter, inducing electricity demand peaks when the heating demand is largest.

To improve the efficiency of air-source heat pumps, one strategy aims at exploiting waste heat streams from domestic hot water usage [7]. Heat recovery at the urban-scale – from the household to receiving

* Corresponding author at: Eawag, Swiss Federal Institute of Aquatic Science and Technology, 8600 Dübendorf, Switzerland.
E-mail address: bruno.hadengue@eawag.ch (B. Hadengue).

https://doi.org/10.1016/j.apenergy.2021.117677
Received 23 April 2021; Received in revised form 22 July 2021; Accepted 20 August 2021
Available online 17 September 2021

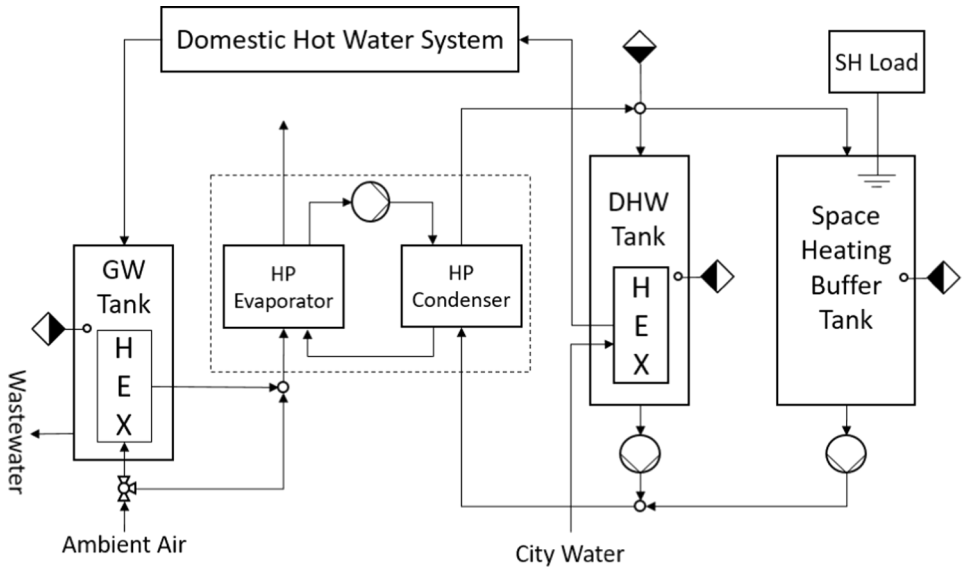

Fig. 1. Schematic description of the heating system with open-loop greywater heat recovery: the air-source heat pump (HP) supplies a domestic hot water (DHW) tank and a space heating (SH) buffer tank. Another tank collects greywater (GW) from the DHW system and a heat exchanger (HEX) preheats the ambient air stream entering the heat pump evaporator.

waters – and its systemic consequences (e.g. on wastewater treatment processes) have been extensively investigated [8–10]. At the level of sewers or wastewater treatment plants, hundreds of full-scale wastewater-source heat pump projects exist around the world [11,12]. In comparison, *building-level* heat recovery has only been gaining traction in recent years. The straightforward use of high-temperature wastewater streams as well as the facilitated local reuse make in-building technologies promising candidates to increase the efficiency of building energy systems [13]. We note, however, the growing concern with regard to competitive interactions between building-level and urban-level heat recovery systems [14,15].

Building-level systems presented in the literature distinguish between passive and active heat recovery. Passive strategies – often referred to as drain water heat recovery – only involve heat exchangers, thus a direct removal of heat from wastewater streams, typically showers [16–20]. Active approaches involve a heat pump in order to further upgrade the recovered heat before reuse. Numerous examples of active heat recovery from wastewater using heat pumps exist in the literature [21–28]. These studies report high potentials for wastewater heat reuse in combination with heat pump systems. However, to our knowledge, few provide comparative results for similar systems using conventional heat sources (e.g., ground, water bodies, ambient air) without wastewater heat recovery. It is thus unclear what efficiency gain can be expected from such systems. Baek et al. [21], for instance, report a coefficient of performance (COP) of 4.5 – 5.0 and 100 % hot water load coverage in a hotel, using a water-water heat pump and greywater as heat source. However, they provide no comparison with an alternative system without heat recovery.

Similarly, Meggers and Leibundgut [25] performed a modeling study on the use of greywater for domestic hot water production with a water-water heat pump, sourcing heat directly from a greywater tank with a heat exchanger incorporated in the tank walls. They argue that high COP values (6 – 7) are feasible by minimizing the temperature lift for the production of 55 °C hot water. The true potential of the heat recovery system is again difficult to assess as no comparison with a conventional heat pump system is provided.

Ni et al. [26], in their modeling study, used greywater stored in an outside tank as a heat source to provide SH and DHW. The authors report a 17 – 57.9 % energy consumption reduction compared to a conventional gas furnace systems in the USA. The benefit of using greywater over a conventional heat pump – e.g., air-sourced –, though, remains unclear.

Postrioti et al. [27], in their experimental study, are among the only authors to provide a comparison with a conventional heat pump system. They used a standard water-brine heat pump in combination with a greywater tank and an outdoor air-unit to provide space heating and domestic hot water. In this study, ambient air temperatures were rather high (around 10 °C) and close to the greywater temperatures. Nevertheless, they report a 12 % COP improvement for the greywater heat recovery system compared to the same system without heat recovery.

In addition to the described lack of comparison with conventional heat pump systems, modeling studies often do not realistically simulate the dynamics of water consumption and water-contained energy (e.g., heat losses from pipes and appliances), which is suspected to affect the assessment of the heat recovery potential [29]. Among the only studies to do so, Seybold and Brunk [28] simulated a water-water heat pump system integrated with a greywater tank to preheat DHW to 45 °C, with an auxiliary gas boiler to heat up DHW to 60 °C. They used real hydrographs to simulate DHW loads and even considered fouling of the heat exchanger in the greywater storage. They report a heat pump COP of 5.5, covering 48 % of the DHW heat demand.

In this paper, we assess the potential of an active greywater heat recovery system to increase the efficiency of air-source heat pumps, as they are the most common type of heat pumps in Switzerland. We use greywater to preheat the airflow entering the heat pump outdoor unit. In contrast with other configurations reported in the literature, we propose an open-loop setup, where an external heat source flow – here ambient air – is preheated before entering the heat pump evaporator. The value of this configuration lies in its simplicity: implementing it in newly constructed buildings or as a retrofit measure to improve the performance of existing air-source heat pumps could be as easy as adding a heat exchanger in series with the outdoor unit.

This study contributes to closing literature gaps detailed in the paragraphs above by analyzing the performance of a greywater heat recovery device under a wide range of scenarios and using realistic simulations of the DHW system. Perhaps most importantly, we compare the heat recovery system with a conventional air-source heat pump system and are therefore able to assess the benefit of upgrading the system with greywater heat recovery. The simulation scenario tree covers three climates, three seasons (winter, fall/spring and summer), two single-family dwellings of different envelope qualities, and two domestic hot water loads. Furthermore, we critically assess the proposed

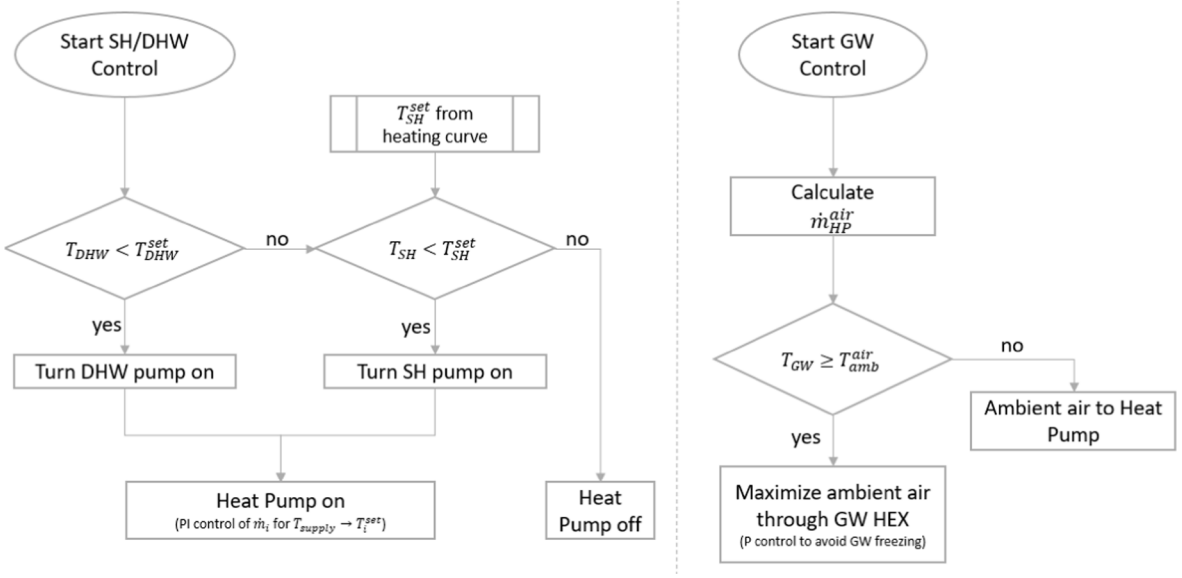

Fig. 2. Flow diagrams of the system operation. Left: heat pump control strategy for the supply of DHW and SH. DHW loads have priority over SH loads. Right: control strategy for the use of greywater (GW) heat, which regulates the mass flow of ambient air through the greywater tank heat exchanger (GW HEX).

Table 1
Selected building archetypes. Characteristics and specific space heating loads.

Building	B1	B2
Type	Residential	Residential
Construction year	2003	1983
Number of floors	3	2
Floor area (m^2)	370.66	405.5
Wall area (m^2)	395.27	352.8
Specific SH load – Geneva (kWh $m^{-2}a^{-1}$)	39.14	88.08
Specific SH load – Rome (kWh $m^{-2}a^{-1}$)	14.73	41.72
Specific SH load – Helsinki (kWh $m^{-2}a^{-1}$)	74.99	153.27

open-loop approach in comparison with closed-loop configurations – using greywater as direct heat source – typically found in the literature and we formulate recommendations for building installation.

2. Materials and methods

2.1. Model description

The modeled system, shown in Fig. 1, includes (i) an air-source heat pump, (ii) a DHW tank, (iii) a SH buffer tank, (iv) a greywater tank and (v) a greywater heat exchanger. The model was programmed in the equation-based modeling language *Modelica* [30], combining the Modelica Buildings Library [31] – for the heating system – and the WaterHub Modeling Framework [32] – for the DHW system. The full model parametrization is available in the supplementary material (Table S1).

We calculated SH loads and DHW loads following methodologies based on building archetypes and DHW systems described in Sections 2.3 and 2.4. Multiple building envelope qualities, climates, and DHW loads were combined into 12 scenarios to determine efficiency gains and energy recovery performances over a wide range of conditions and setups.

2.2. System operation

Flow diagrams in Fig. 2 describe the operation strategies. The heat pump operates with priority on DHW over SH, thus turning the heat pump on when the DHW tank temperature falls below a threshold T_{DHW}^{set}, set to 60 °C (with a bandwidth of 12 K, i.e. turning the heat pump on when the tank temperature falls below 54 °C and off when reaching 66 °C), in accordance with guidelines provided by SVGW [33] for the prevention of *Legionella* growth in DHW systems. If no DHW recharge is required, the SH operation turns the heat pump on when the temperature of the SH buffer tank falls below a threshold T_{SH}^{set}, based on the building's heating curve (see Section 2.3 and Appendix B). The operation of the active heat recovery system aims at maximizing the airflow through the heat exchanger connected to the greywater tank, under the condition that the greywater in the tank is both warmer than ambient air and above 0.2 °C to prevent freezing in the greywater tank.

2.3. Space heating load

We simulated two single-family homes (SFH) with different SH loads, representing two buildings of different age classes and envelope qualities. The selected SFHs both featured a floor area of 141 m^2, representing the statistical mean size of a SFH in Switzerland [34]. We calculated SH loads based on two sample buildings selected from a set of building archetypes representing the Swiss residential building stock [35]. Table 1 summarizes their main characteristics as well as specific heating loads simulated with EnergyPlus [36] for three selected climates: Geneva, Switzerland (temperate), Rome, Italy (Mediterranean) and Helsinki, Finland (humid continental). In Geneva, the selected buildings showed an annual specific heating load of 39.14 and 88.08 kWh m^{-2} a^{-1}. With moderate space heating intensities, both buildings qualified for floor heating and heat generation by means of an air-source heat pump. For each simulation, we calculated absolute SH loads by normalizing the climate- and building-dependent specific SH load to 141 m^2.

The model does not simulate the building's heat emission system directly (in this case a radiant floor heating system). Instead, calculated SH loads were connected – thermally – to the SH buffer tank. Thus, besides SH loads, the model required supply temperatures for a virtual floor heating system. Supply temperatures are crucial for the performance of the heat pump as they directly influence the heat pump temperature lift. We determined the supply temperature as a function of the ambient air temperature, i.e. the heating curve of the building, following a methodology adapted from Rhee et al. [37]. The method estimates the supply temperature required to meet a given floor surface temperature based on the assumption that the building has a single zone (no internal partition). A full description of this method is available in Appendix B. As heating curves were similar for all climates, the Geneva heating curves – one for B1, one for B2 – were used in all scenarios.

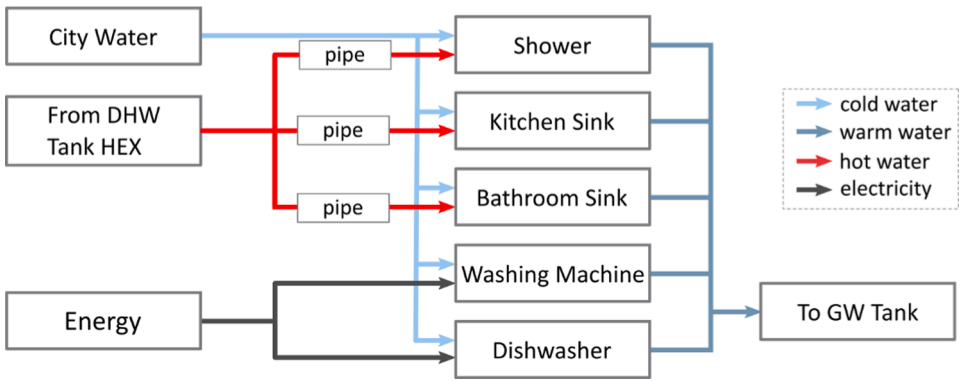

Fig. 3. Greywater system appliances and plumbing layout, modeled with the WaterHub modeling framework [29]. The hot water flows from the domestic hot water tank heat exchanger (DHW Tank HEX).

Table 2
Water consumption events for the greywater-producing appliances. We give values for flow, temperature and total volume distribution. The total consumption column describes Swiss averages.

Appliance	Single Event Characteristics				Total Consumption[38]
	Flow [L/s]	*Temperature [°C]*	*Total Volume [L/event]*	*Reference*	*Volume [L/cap day]*
Shower	N(0.183, 0.042)	N(36.0, 4.09)	N(43.9, 33.7)	[39]	37
Kitchen sink	0.08	35	1.2	[41]	21
Bathroom sink	0.04	35	1.6	[41]	15
Washing machine	0.17	37	10.2	[41]	18
Dishwasher	0.08 (Wash)	655,045	4.8	[41,44]	3
	0.06 (Cold rinse)		3.6		
	0.07 (Hot rinse)		4.2		

As a consequence of not simulating the heat emission system directly, the SH loads follow ambient conditions, hence not capturing the full dynamics of the building heating demand. However, the addition of a SH buffer tank in the system mitigates this effect by simulating the thermal mass of the heat distribution system. Because the heat recovery system interacts only with the DHW system, the simulated dynamics of heat demand for SH are sufficient for a good estimation of the heat recovery performance.

Based on the climate and building archetypes – i.e. SH loads and heating curve –, we sized the SH system by parametrizing the heat pump model (i.e. nominal compressor power, nominal COP) and selecting a SH buffer tank size with enough thermal capacitance to mimic the building thermal capacitance, which we do not simulate directly. We give the full details of the heat pump parametrization in Appendix C.

2.4. Domestic hot water system

We modeled the DHW system using the Modelica WaterHub Library [29]. The library contains models for appliances, water pipes and interface models for compatibility with the Modelica Buildings Library [31]. Fig. 3 shows the DHW system model. The DHW system reflects greywater-producing appliances found in typical Swiss SFHs: a shower, a kitchen tap, a bathroom tap, a washing machine and a dishwasher. Details of the parametrization of the DHW system are given in the supplementary material in Table S1.

Switzerland's water demand is on average 142 L per person per day, of which 42 L is for toilet flushing and 37 L for showering [38]. To simulate the water consumption of each appliance producing greywater, we performed Poisson processes on appliance-resolved consumption curves and event profiles provided in the literature, which we scaled to Swiss averages (see Table 2) [39–44]. Although the consumption

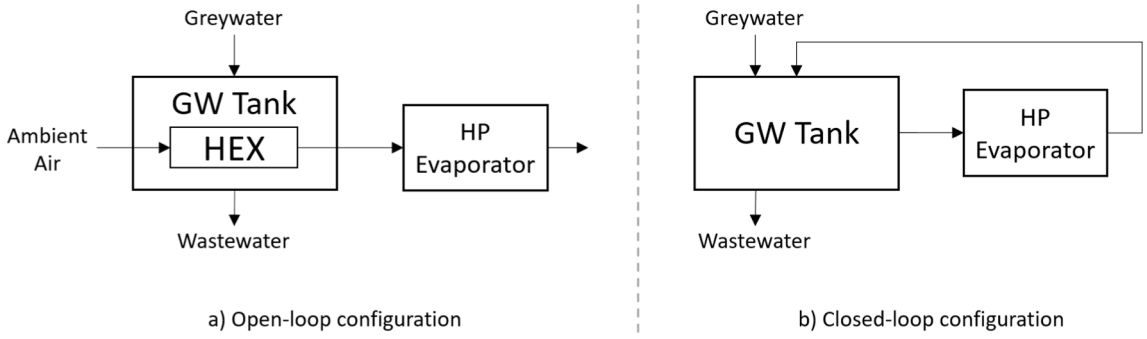

Fig. 4. Open- vs. closed-loop heat pump configurations for greywater (GW) heat recovery: a) in the open-loop configuration, the greywater is used to preheat the heat source flow – here ambient air – with a heat exchanger (HEX) before entering the heat pump evaporator. The flow leaving the evaporator is not fed back into the system. b) In a closed-loop system, the greywater is used directly as a heat source and the return flow is fed back into the greywater tank. Details of open- and closed-loop implementations are shown in Fig. 1 and Fig. 10 (Appendix D), respectively.

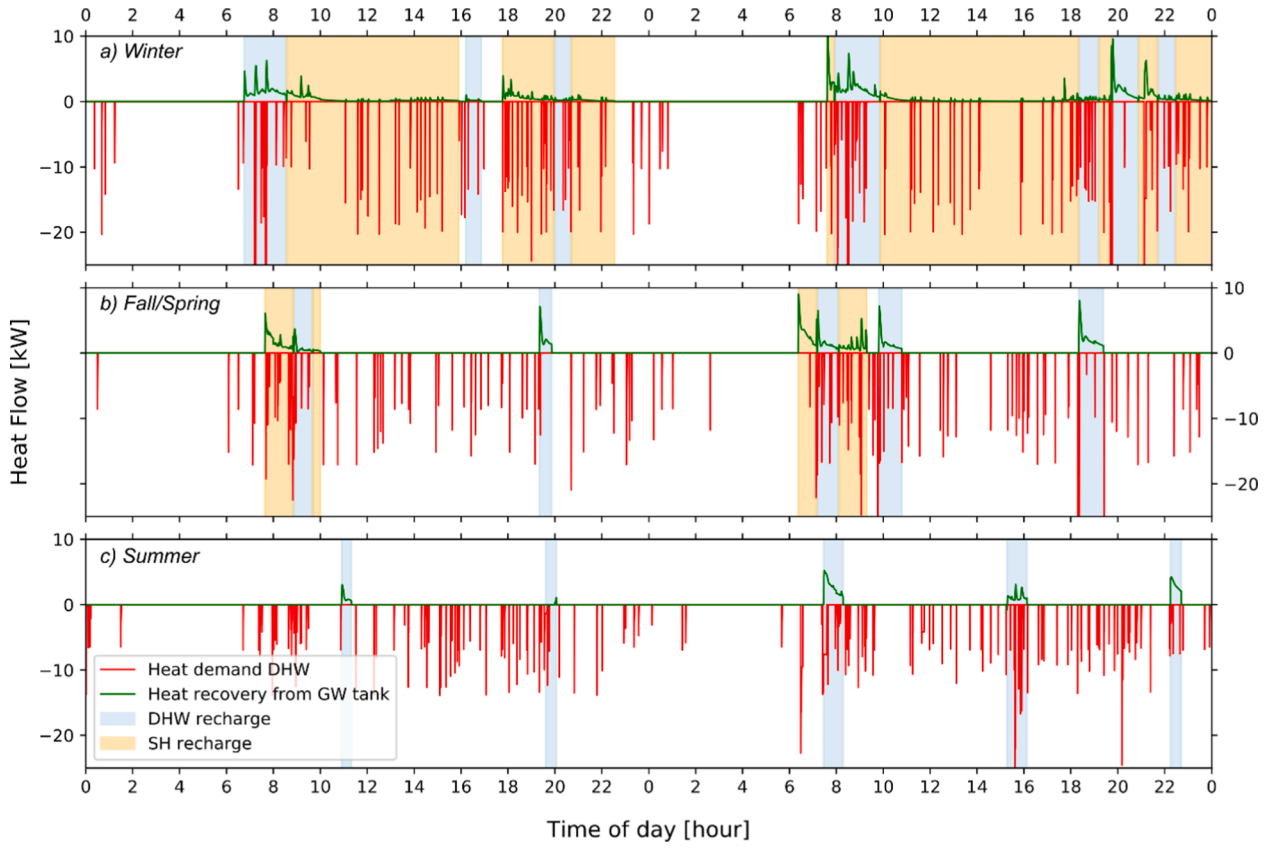

Fig. 5. Simulation output example of the open-loop heat recovery system for two consecutive days in winter (a), fall/spring (b) and summer (c), for the scenario (Geneva – B1 – Low DHW). The curves show the stochastic DHW heat demand and the related heat recovery power during heat pump operation periods. Spikes in heat recovery power appear after large DHW events – for instance showers. Heat recovery power is decaying fast (1–2 h), as the temperature in the greywater tank decreases.

schedules found in the literature describe UK households, we expect the water consumption habits of Swiss and UK inhabitants to be similar.

In order to evaluate the effect of water consumption loads on the heat recovery system, we considered two household compositions. Swiss SFHs are, on average, inhabited by 2.6 people [34]. The first "low consumption" household composition thus included two adults and one child (consuming 60 % of an adult's water consumption). A second "high consumption" composition simulated the water consumption of five adults (i.e. roughly twice the low water consumption).

2.5. Simulations

In total, three climates (Geneva, Rome and Helsinki), two buildings (B1 and B2), and two domestic hot water loads ("high" and "low") formed a scenario tree with twelve distinct scenarios. In this main simulation round, we simulated three weeks for each scenario: a winter week (coldest of the year), a summer week (warmest of the year) and a fall/spring week (median week). One simulation week consisted of eight consecutive simulation days, allowing the system to reach a steady state during the first day before logging simulation results for the following seven days. Time resolution was set to 10 s, a fair compromise to account for short water consumption events while not surrendering computational efficiency. We replicated each simulation 20 times (140 days) to account for the stochastic nature of domestic hot water consumption.

From the raw simulation outputs, we computed the weekly average COP of the heat pump during DHW, SH, and total (DHW *and* SH) operation. We then compared systems supported by greywater heat recovery to their reference counterpart (i.e. systems operating without heat recovery) and derived the respective COP increase and weekly electricity savings.

2.6. System setup comparison

Following the main simulation round covering the 12 scenarios described above, we performed additional simulations of a system under various configurations (open/closed-loop) using (Geneva – B1 – Low DHW) as a reference scenario. As visualized in Fig. 4, open-loop systems refer to the pre-heating of an external heat source – here ambient air – using greywater, while closed-loop systems use greywater as direct heat source. Similar to the main simulation round, each configuration was simulated for winter, fall/spring and summer weeks, and was simulated 20 times. The four configurations tested were (i) open-loop mixed mode, (ii) open-loop DHW mode, (iii) open-loop SH mode and (iv) closed-loop for DHW production only:

(i) *Open-loop mixed mode*: main simulation round as described in Section 2.5; the heat recovery system supports the heat pump during both DHW and SH operation.
(ii) *Open-loop DHW mode*: the heat recovery system supports the heat pump only during DHW operation and not SH operation.
(iii) *Open-loop SH mode*: the heat recovery system supports the heat pump only during SH operation and not DHW operation.

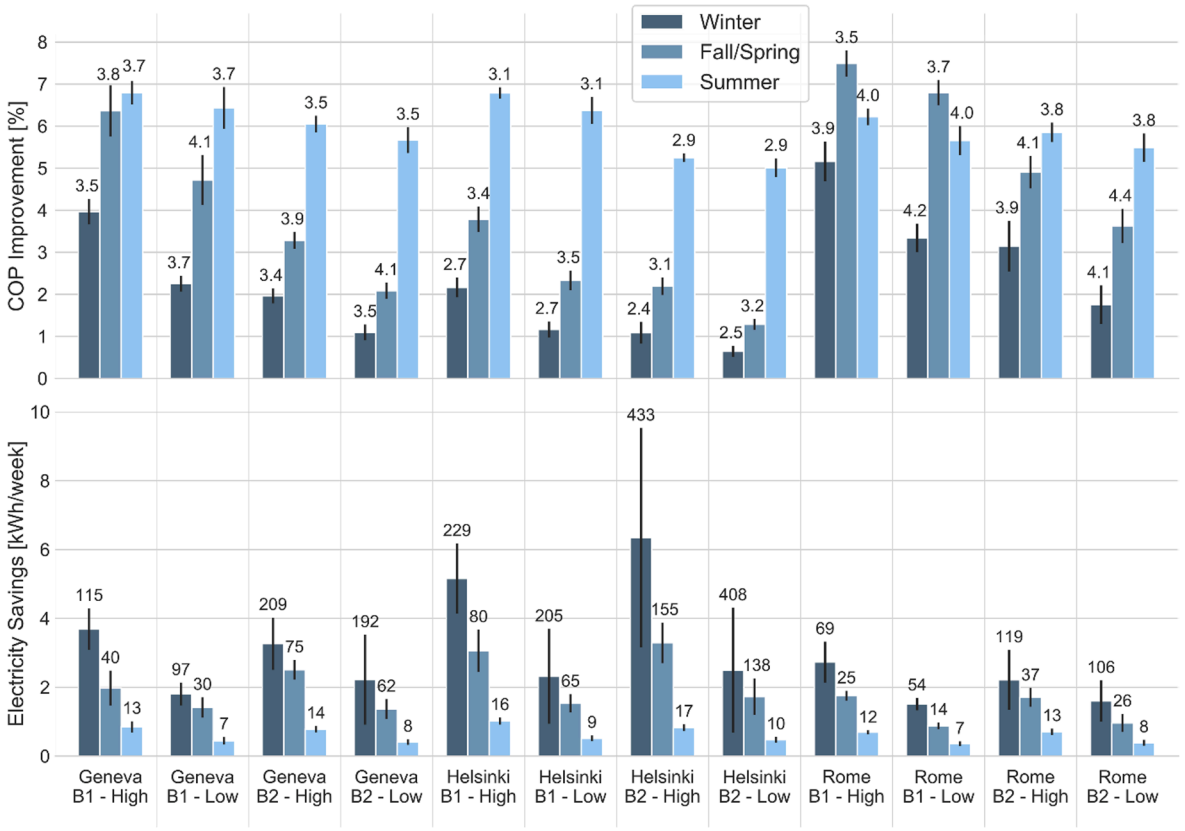

Fig. 6. Top: COP improvements with weekly standard deviations. Labels on top of each bar indicate the COP of the reference system (without heat recovery). Bottom: weekly average electricity savings in kWh and weekly standard deviations. Labels indicate the electricity consumption of the reference system in kWh/week.

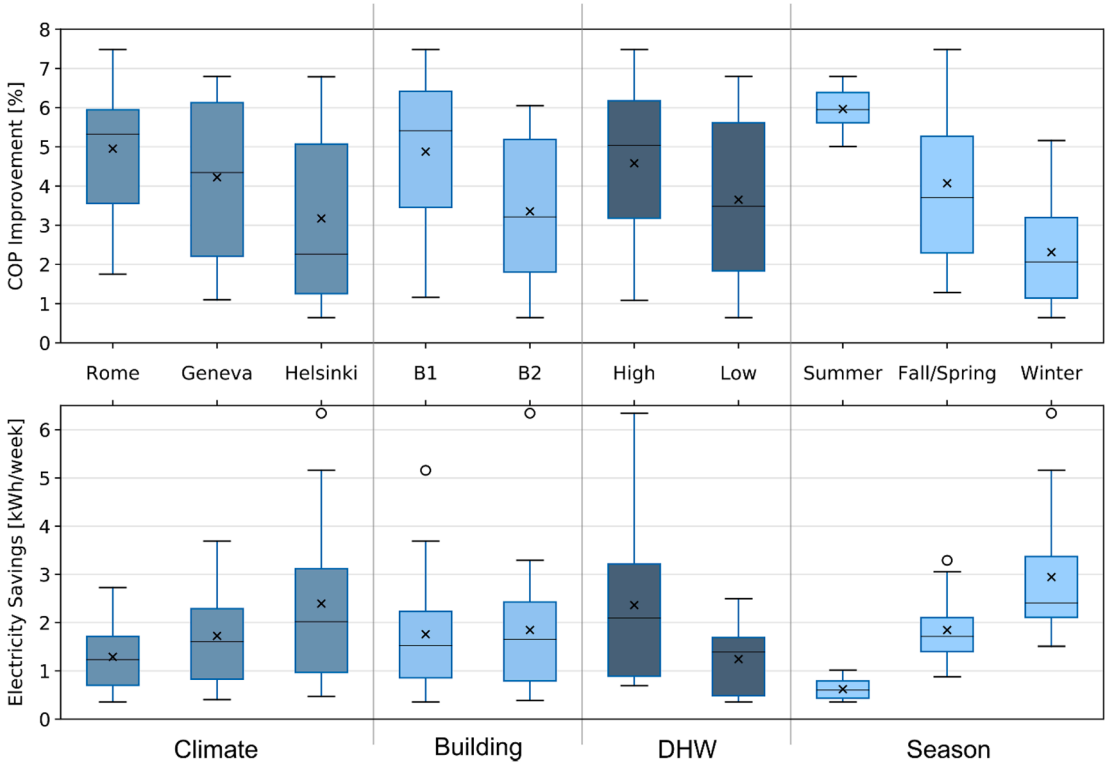

Fig. 7. Factor-resolved distributions for COP improvements (top) and electricity savings (bottom). Lines and crosses show median and average values, respectively. Warmer conditions (Rome and summer weeks) and better performing buildings (B1) induce the largest COP improvements in the system, although the largest electricity savings occur in colder climates (Helsinki and winter weeks) and worse performing buildings (B2).

Table 3
Summary of COP values for (Geneva - B1 - Low DHW). In brackets: increase relative to the reference system (single air source heat pump - no heat recovery).

Geneva Building 1 Low DHW	*Operation*	Open-Loop Mixed Mode	Open-Loop DHW Mode	Open-Loop SH Mode	Closed-Loop + air-source HP for SH
Winter	DHW + SH	3.81 *(+2.3%)*	3.81 *(+2.3%)*	3.81 *(+2.1%)*	*3.89 (+4.4%)*
	DHW	2.75 *(+4.9%)*	2.89 *(+10.1%)*	2.62 *(+0.0%)*	3.31 *(+26.4%)*
	SH	4.12 *(+1.5%)*	4.06 *(+0.1%)*	4.17 *(+2.7%)*	*4.06 (+0.0%)*
Fall/Spring	DHW + SH	4.25 *(+4.7%)*	4.27 *(+4.4%)*	4.25 *(+4.1%)*	*4.37 (+6.8%)*
	DHW	3.20 *(+6.5%)*	3.29 *(+9.5%)*	3.01 *(+0.0%)*	3.59 *(+19.0%)*
	SH	5.26 *(+3.2%)*	5.10 *(+0.0%)*	5.52 *(+8.2%)*	*5.10 (+0.0%)*
Summer (no SH)	DHW	3.95 *(+6.4%)*	3.96 *(+6.5%)*	3.67 *(+0.0%)*	3.97 *(+7.3%)*

(iv) *Closed-loop (DHW only)*: similar to Meggers and Leibundgut [25], a closed loop of water thermally connects the greywater tank with the heat pump evaporator for the production of DHW only. A schematic of the system is provided in Appendix D. (Fig. 10). Here, an additional air-source heat pump provides SH loads.

Similarly to the main simulation round, we computed the weekly average COP of each configuration during DHW, SH, and total (DHW *and* SH) operation. We compared these values to the reference system, i.e. the conventional air-source heat pump, as well as with COP values from the various setup configurations tested in the literature. For the closed-loop case, we computed the average COP for total operation (DHW + SH) assuming that the relative weight given to each operation was identical to the open-loop mixed mode setup.

3. Results

Fig. 5 shows an example of a simulation output of heat recovery dynamics for the scenario (Geneva – B1 – Low DHW) during two consecutive days in winter, fall/spring and summer. In this example, the heat pump is turned on roughly 65 % of the time in winter for the production of SH and DHW, 20 % in fall/spring and only 5 % in summer (no SH loads). After long periods where the heat pump is not in use or after energy-intensive DHW events (for instance morning showers), heat recovery is at its maximum with the greywater tank charged with hot, freshly produced greywater. When the heat pump is then switched on, heat recovery power rapidly decays to zero – typically within one or two hours – as the temperature in the greywater tank falls below that of ambient air and the heat recovery system becomes inoperative.

3.1. Open-loop system performance

We show COP improvements and weekly electricity savings for the twelve scenarios of the main simulation round (open-loop configuration) in Fig. 6. COP improvements range from 0.6 % (Helsinki – B2 – Low DHW – winter) to 7.5 % (Rome – B1 – High DHW – summer). The scenario average improvement is 4.1 %. Net weekly electricity savings average 1.8 kWh/week over all scenarios, with a maximum of 6.3 kWh/week (Helsinki – B2 – High DHW – winter) and a minimum of 0.4 kWh/week (Rome – B1 – Low DHW – summer).

The heat recovered in the system is not shared equally for the support of DHW and SH operation. On average, across all scenarios, 69 % of the recovered heat supports DHW operation (31 % for SH operation), leading to an overall COP improvement of 5.5 % for DHW operation and 2.0 % for SH operation. In winter, however, the system uses recovered heat more equally for the support of the heat pump: 47 % is used for DHW and 53 % for SH operation.

Fig. 7 shows factor-resolved distributions of the results, confirming performance patterns already visible in Fig. 6: on average, we report better COP improvements in warmer conditions (summer or Rome, respectively 6.0 % and 5.0 %) and better performing buildings (B1 – 4.9 %), as well as higher DHW loads (high DHW – 4.6 %). In contrast, simulations of colder climates (winter or Helsinki, respectively 2.3 % and 3.2 %) or worse performing buildings (B2 – 3.4 %), as well as lower DHW loads (low DHW – 3.7 %) yield lower COP improvements but generally higher absolute electricity savings, above the 2 kWh/week mark.

An analysis of variance confirms the prominent role of the season: 54 % of the COP improvement variance is explained by the seasonal factor ($p < 0.05$), the other factors having significant but less determinative roles (14 %, 13 % and 5 % of the variance explained by the factor building, climate, and DHW, respectively, with $p < 0.05$). The analysis of electricity savings provides similar insights – the seasonal factor explaining most of the results' variance (51 %) – with the notable difference that the building factor becomes insignificant (p greater than 0.05).

3.2. System setup comparison

In an attempt to reconcile the results with the literature values and to

Table 4
Literature comparison.

Study	Setup Configuration	Key Findings
[21]	Closed-loop greywater heat recovery for DHW production in a hotel (50 °C)	COP: 4.5 – 5.0 100% DHW load coverage
[25]	Closed-loop greywater heat recovery for DHW production (55 °C)	COP: 6.0 – 7.0 100% DHW load coverage
[26]	Closed-loop greywater heat recovery with external air as auxiliary source for DHW, SH and cooling	COP: not communicated 17% – 57.9% source energy reduction compared to gas-fired boiler
[28]	Closed-loop greywater heat recovery for DHW production (45 °C) with auxiliary gas boiler up to 60 °C	COP: 5.5 48% DHW load coverage
[27]	Closed-loop greywater heat recovery with air-source heat pump for DHW and SH	COP: 3.72 12% COP increase compared to air-source heat pump
This study	Open-loop greywater heat recovery with air-source heat pump for DHW and SH	COP: 2.48 – 4.55 0.6% – 7.5% COP increase compared to air-source heat pump

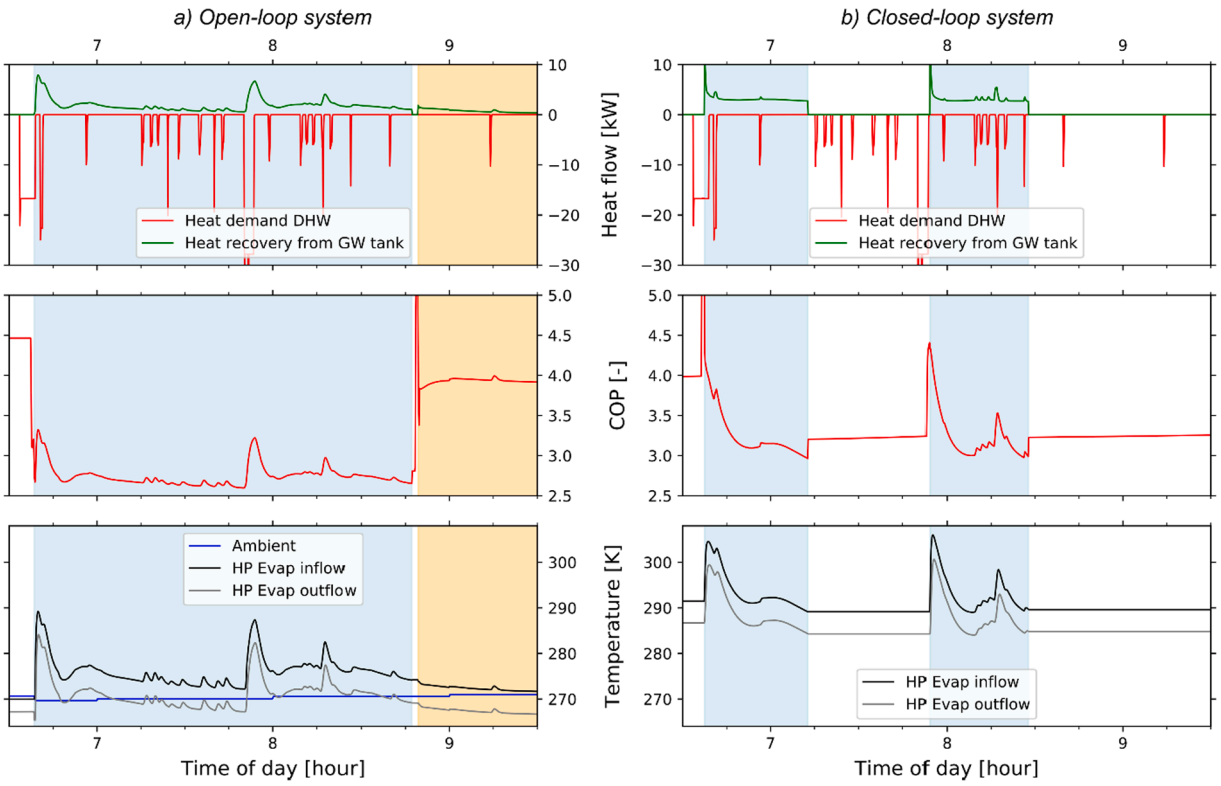

Fig. 8. A close-up view of system dynamics for (a) an open-loop system and (b) a closed-loop system in Geneva (Building 1 – Low DHW - winter). Light blue shaded areas represent DHW operation and orange SH operation (only for the open-loop system). (For interpretation of the references to colour in this figure legend, the reader is referred to the web version of this article.)

Table 5
Summary of key values for the determining of heating curves in Geneva, for the two buildings B1 and B2.

	$T_{amb}^{min1\%}$ [°C]	$Q_{design}^{min1\%}$ [kW]	$q_{design}^{min1\%}$ [Wm^{-2}]	K_{design} [Wm^{-2}K^{-1}]	α
Building 1	−2.9	3.33	23.60	5.62	1.233
Building 2		5.32	37.73	5.0062	1.618

investigate the influence of system setup on the heat recovery performance, we simulated scenarios (Geneva – B1 – Low DHW) in various system configurations: (i) open-loop mixed mode (as presented in Section 3.1), (ii) open-loop DHW mode, (iii) open-loop SH mode, and (iv) closed-loop for DHW operation, complemented with an air-source heat pump for space heating. We report average COP values in Table 3. Results from DHW operation show that the closed-loop configuration clearly outperforms open-loop configurations with the exception of the summer period, for which we report similar COP values (3.95 – 3.97, leaving out the "SH mode" configuration as heat recovery is inoperative).

As we include SH operation in the comparison, results tend to be

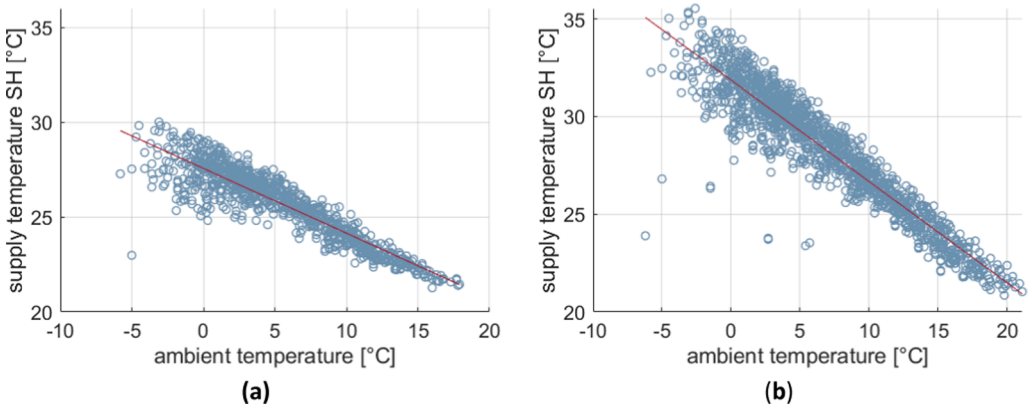

Fig. 9. Scatter plot of filtered supply temperature data (blue) and linear trend (red) evaluated for Geneva, Switzerland: (a) Building 1 and (b) Building 2. (For interpretation of the references to colour in this figure legend, the reader is referred to the web version of this article.)

more homogenous: the closed-loop configuration – complemented with an air-source heat pump – shows for instance a COP of 3.89 in winter, which is closer to COP values displayed by open-loop configurations (3.81). The same is true for the fall/spring period (4.37 and roughly 4.25 for closed-loop and open-loop configurations, respectively).

4. Discussion

4.1. Open-loop system

The open-loop implementation for greywater heat recovery, as presented in Section 3.1 above, shows limited potential, with only 4.1 % COP improvement and 1.8 kWh/week electricity savings over the range of scenarios studied. The improvement is low because the achieved temperature increase at the inflow of the evaporator is limited: the time-averaged temperature is only 2.7 K higher than ambient air temperature during heat pump operation. Compared to typical temperature lifts (e.g., roughly 30 K for SH in fall/spring, up to 70 K for DHW in winter) in the air-source heat pump, the pre-heating step provides only a marginal performance benefit.

Source- and temperature-limitation effects are at the core of the heat recovery dynamics and explain the low potential of this technology. To exemplify these effects, we look at two operation modes simulated for scenario (Geneva – B1 – Low DHW), whose results are presented in Table 3: (i) DHW mode, where the recovered heat supports only DHW operation, and (ii) SH mode, where the recovered heat supports only SH operation. (i) In DHW mode, enough heat is recovered from the greywater tank to provide a significant air temperature increase at the inflow of the heat pump evaporator. During DHW operation, the average temperature increase is 7.4 K in winter and 6.3 K in fall/spring, thus substantially larger than the 2.7 K increase reported above in mixed mode. However, temperature lifts during DHW operation are large: roughly 65 K in winter and 55 K in fall/spring, reducing the effect of larger air temperature increases on the heat pump COP. (ii) In SH mode, temperature lifts are smaller, typically in the range of 20–35 K. However, the system is now strictly source-limited: SH loads are larger than DHW loads by a factor 5 in winter and by a factor 2 in fall/spring. Consequently, the average air temperature at the evaporator inflow only increases by 1.3 K and 3.4 K, respectively, leading to low COP improvements.

The balance between source- and temperature-limitation effects explains factor-resolved results in Fig. 7. Warmer conditions (climate or season) and better buildings – with small SH loads – lower the magnitude of the source-limitation effects, thus increasing COP improvements. Similarly, high DHW loads partly mitigate source-limitation effects and COP improvement increases. In contrast, temperature-limitation effects favor colder conditions (climate or season): more heat can be recovered from the greywater tank in low ambient air temperatures, inducing larger absolute electricity savings.

4.2. Literature comparison

Comparing open-loop system results with the existing literature is not straightforward as it is uncommon for articles to report on the efficiency gain of the wastewater heat recovery system compared to a heat pump unsupported by heat recovery. Rather, comparisons with conventional systems are presented (e.g., a gas-fired boiler in Ni et al. [26]. In addition, other (simulation) studies do not report on a wide range of scenarios as we do here. It is thus difficult from these publications to analyze the impact of individual factors, such as climate or building performance, and thereby hypothesize where and how the implementation of such heat recovery systems would be most sensible. Lastly, fundamental differences in setup – open- vs closed-loop systems being the most striking – and heterogeneous assumptions/boundary conditions make the comparison more difficult. We attempt to analyze and reconcile the results in the following paragraphs.

At first glance, the large discrepancies between results reported in the sections above and some values found in the literature are striking. We provide a summary of key findings from various studies in Table 4. With our scenario-average COP of 3.69, our estimated COP is lower than most reported values in the literature (most reported COPs ranging from 4.5 to 7.0), with the exception of Postrioti et al. [27].

Ni et al. [26] report 57.9 % energy savings compared to a conventional gas furnace in Bellingham, WA, a climate very similar to Geneva (temperate oceanic). If we were to compare our results for Geneva - B2 (average COP 3.79) to the same gas-fired system (efficiency 0.80, source energy conversion factor 1.088), it would result in a 64.9 % energy saving, assuming the same source energy conversion factor for electricity as for Bellingham (1.807). Taking potential minor climate variations into consideration, our results are thus in close agreement. We note, though, that this comparison prevents distinguishing the benefit of the heat recovery system relative to a standard air-source heat pump installation as we can safely argue that the latter is responsible for most of the reported energy savings when compared to a gas furnace.

The experimental system analyzed by Postrioti et al. [27] and our scenario (Rome – B1 – fall/spring) have similar boundary conditions (ambient temperatures and building type). Reported COP values in both studies are thus in close accordance (3.67 versus 3.65, respectively), although we compute slightly different COP improvements (12 % in Postrioti et al. [27], 8.0 % in this study). This difference is likely to stem from the heterogeneous DHW consumption data and other setup differences such as heat pump characteristics.

Larger discrepancies arise when comparing our results with other closed-loop systems. Baek et al. [21] report a COP range of 4.5 – 5.0, while Seybold and Brunk [28] report a COP of 5.5, and Meggers and Leibundgut [25] report COP values as high as 6.0 – 7.0. We claim that, besides the differences in system topologies (open vs. closed-loop, described below in Section 4.3), much of the difference stems from different choices in boundary conditions and assumptions. First, these studies focus only on the production of DHW, leaving SH aside. Second, DHW is produced at lower temperatures (45 – 55 °C) compared to our system where the supply temperature of the DHW tank is 66 °C and temperature differences across heat exchangers are only partly considered. Lastly, our system considers dynamic processes inherent to DHW consumption: first, heat losses from the piping layout in the DHW system likely influence greywater temperatures and thus reduce overall efficiency. Second, the stochastic DHW consumption drives recharge patterns of the greywater tank as well as operation schedules of the heat pump, which is likely to influence the overall system efficiency. When using identical boundary conditions to compare a closed-loop system and an open-loop system, as shown in Table 3, differences in COP values are much smaller, showing the influence of boundary conditions and other assumptions made as part of a given study.

4.3. Open- vs. closed-loop systems

Regardless of boundary conditions and other assumptions, the system configuration plays a major role in the performance of the heat recovery system. There are fundamental differences between the two configurations, reflected in the performance data presented in Table 3.

In an open-loop system, the ambient air stream is first preheated by the greywater heat source. Then, in the heat pump evaporator, the fraction of heat removed from the air stream depends on the constant design temperature difference across the evaporator. Thus, when the temperature increase in the preheater is larger than the design temperature difference of the evaporator, the heat pump uses only a portion of the recovered heat. As the unused heat is not fed back into the system, it is lost to the environment and the greywater tank consequently quickly cools down. On average, in mixed mode, 12 % of the recovered heat is subsequently lost to the environment after the evaporator (range 5 – 25%). In DHW mode, though, the share of lost energy increases up to 40 % in winter, since the heat recovery system operates mostly for short periods at high temperature.

It would be straightforward to optimize the control of the preheating step to exactly match the temperature difference at the evaporator, thus mitigating heat losses. In this case, the airflow temperature increase would be reduced but could be sustained for a longer period. However, we expect this optimized control to improve the system only marginally due to the source-limitation in mixed and SH mode, combined with generally smaller temperature increases.

A further feature of the open-loop configuration is the dependence of the heat recovery power curve on the greywater temperature. As greywater gradually cools down, the temperature difference between greywater and ambient air, and with it the heat recovery power, decreases. We observe clearly, in Fig. 8, the above-described behaviors of unused recovery potential being lost and quickly decreasing discharge power. The temperature curves show, for the first 15 minutes of heat pump operation, high air temperatures at the entrance of the evaporator, quickly decreasing to levels close to ambient. The heat recovery curve shows a similar pattern.

In contrast to the open-loop behavior, the closed-loop configuration feeds unexploited heat at the evaporator back into the system. The evaporator and the greywater heat exchanger thus both operate at a constant temperature difference leading to constant heat recovery power. The greywater temperature gradually declines as the evaporator removes heat from the water flow, but since there is no loss to the environment, the discharge is more continuous and significantly slower. The power curve in Fig. 8 shows continuous heat recovery power during the entire DHW operation event of about 40 min, resulting in shorter DHW operation periods compared to the open-loop configuration.

In addition, the temperature curves generally show higher values at the evaporator inflow for the closed-loop setup. Indeed, a further difference between the two configurations relates to the climate-dependence of the open-loop system. In this configuration, evaporator temperatures result from the ambient temperature plus the temperature increase achieved by heat recovery, making it very responsive to climate variations. The highest heat recovery performance is achieved at high ambient temperatures, when the temperature increase achieved in the pre-heater better matches the temperature difference across the evaporator and less of the heat potential added to the air stream is lost to the environment. However, high ambient temperatures also increase the heat pump performance: the relative performance increase during warmer periods is thus smaller than during colder periods (Table 3).

In contrast, the closed-loop configuration is much less climate dependent. During warmer periods, DHW loads decrease due to the warmer city mains. DHW operation periods are thus shorter, increasing the average COP.

4.4. System integration

We selected the open-loop setup for its suitability as an easy and inexpensive retrofitting option for existing air-source heat pump systems, as these are most common in Switzerland. The implementation of such a greywater heat recovery system only requires a greywater tank and an additional water/air heat exchanger to preheat the ambient air stream before it enters the heat pump evaporator. However, our analysis showed that performance improvements are moderate, and we can argue that the greywater separation in an existing building is challenging and would thus be feasible only for deep retrofitting projects. Such cases, though, require major adjustments of the building system, potentially justifying the implementation of a closed-loop approach instead.

The closed-loop configuration outperformed open-loop configurations and led to a significant performance increase, especially in colder climates. However, its integration is more challenging. This configuration can be implemented in many different ways, as shown by Meggers and Leibundgut [25], Ni et al. [26], Postrioti et al. [27], Seybold and Brunk [28]. Meggers and Leibundgut [25], for instance, assess the performance of a dedicated heat pump for DHW production. Consequently, a separate heat pump for space heating would be required. We follow a similar approach in our system setup comparison as we assume a separate air-source heat pump for space heating (Table 3). Alternatively, multi-source approaches as presented by Ni et al. [26] or Postrioti et al. [27] can be operated with a single heat pump, serving both SH and DHW.

Overall, we claim that there are cases where the implementation of in-building active heat recovery is reasonable and may lead to a significant performance increase. In locations where better heat sources than ambient air – such as the ground – are exploitable, greywater heat recovery is not beneficial. When used in combination with air-source heat pumps and, even more, when hot water consumption is comparatively large, there are evident benefits to implementing greywater heat recovery. Interestingly, this is not only true from an energy perspective but also from a resource perspective: in-building greywater separation, treatment and exploitation is being increasingly researched and implemented around the world [45]. We anticipate that natural synergies will emerge between decentralized greywater treatment and heat recovery technologies since they may share some attributes, for instance the need for a greywater storage tank. More generally, we note that in-building heat recovery must be embedded carefully in the surrounding energy system. Future research should aim at integrating the technologies discussed in this study optimally with existing neighborhood- or urban-level technologies, for instance in the context of low-exergy design principles [46] or else in the context of heat recovery at the urban-level [14,15].

5. Conclusions

We tested an open-loop greywater heat recovery system – preheating of the air stream for an air-source heat pump – over a wide range of climates, buildings, domestic hot water loads, and seasons. Although attractive due to system simplicity and the potential for the retrofitting of existing buildings, the potential of this heat recovery configuration is generally low (0.6 % to 7.5 % COP increase – 0.2 to 6 kWh/week electricity savings, depending on the conditions). Warmer climates and better buildings induce larger coefficient of performance improvements. Colder climates and increased domestic hot water consumption induce larger overall electricity savings.

Additionally, we extended the scenario analysis by comparing two system configurations – open- and closed-loop – for active heat recovery and we identified fundamental differences in heat recovery dynamics and climate dependence. Closed-loop configurations clearly outperform open-loop configurations for the production of domestic hot water in buildings.

In alignment with findings from literature, we claim that closed-loop systems should be considered for implementation in buildings with comparatively large domestic hot water consumption (hotels and swimming pools, for instance) despite being more expensive and more complex than open-loop configurations. In regular apartment buildings, closed-loop heat recovery could lead to energy efficiency gains, particularly for well-performing buildings and in cold climates, and possibly also in the future in synergistic combinations with decentralized grey-water treatment technologies.

CRediT authorship contribution statement

Bruno Hadengue: Conceptualization, Methodology, Software, Investigation, Visualization, Writing – original draft. **Eberhard Morgenroth:** Supervision, Writing – review & editing. **Tove A. Larsen:** Conceptualization, Supervision, Writing – review & editing. **Luca Baldini:** Conceptualization, Supervision, Methodology, Investigation, Writing – review & editing.

Declaration of Competing Interest

The authors declare that they have no known competing financial interests or personal relationships that could have appeared to influence the work reported in this paper.

Acknowledgements

This research project is financially supported by the Swiss Innovation Agency Innosuisse and is part of the Swiss Competence Center for Energy Research for Efficiency in Industrial Processes (SCCER EIP) (contract number 1155002538).

Appendix A. Supplementary material

Supplementary data to this article can be found online at https://doi.org/10.1016/j.apenergy.2021.117677. The source code and raw data can be found online at https://doi.org/10.25678/00042K.

Appendix B. Heating curve

To determine the supply temperature as a function of ambient air temperature, i.e. the heating curve of the building, we adopted a methodology proposed by Rhee et al. [37]. Assuming the building represents a single thermal zone without internal partitions, the supply temperature for the space heating depending on ambient air temperatures can be expressed as

$$T_{supply} = T_{room} + \left[\frac{\alpha \sum\left(U_i A_i + \dot{V}_{air}\right)}{\dot{m}_w c_w}\right](T_{room} - T_{ambient}) = T_{room} + \alpha \frac{\dot{Q}_{sh}(T_{ambient})}{\dot{m}_w c_w} \quad (1)$$

where $U_i A_i + \dot{V}_{air}$ is estimated from the simulated hourly space heating demand divided by the temperature difference $T_{room} - T_{ambient}$ and α is a coefficient representing the geometry and thermal property of the radiant floor, which we calculate as

$$\alpha = \left(1 - \exp\left(-\frac{A_f B \prod_i (a_i^{m_i})}{m_w c_{p,w}}\right)\right)^{-1}. \quad (2)$$

Here, A_f represents the floor area, B a heat exchange coefficient, and the power product is specific to the floor heating installation (including pipe diameter, spacing, floor covering, etc.). m_w represents the mass flow and $c_{p,w}$ the specific heat of the water circulating in the floor heating.

In order to calculate α, we followed the following procedure:

- We compute $T_{surf,ave}$ using the basic equation $q = 8.91*(T_{surf,ave}\text{-}T_{room})^{1.1}$ according to DIN EN 1264–2 [47]. Here, $T_{surf,ave}$ is set to meet the design heat load, assuming a design room temperature of 20 °C.
- The design heat load Q_{design} is evaluated by calculating the space heating load for a specified external design temperature T^{air}_{design}. We selected T^{air}_{design} based on the climate data/weather file to be the temperature that is below 99 % of recorded ambient temperatures. It thus excludes the extreme 1% of ambient temperatures.
- We assume plaster/screed integrated floor heating, with a 0.04 m layer and a thermal conductivity of 1.2 W $m^{-1}K^{-1}$ above the heating tubes, with wooden floor covering of 0.015 m and a thermal conductivity of 0.15 W $m^{-1}K^{-1}$ to calculate average water temperature expressed as the arithmetic average of $(T_{supply} + T_{return})/2$. Using a design temperature difference of 7 K, we calculate the design mass flux and T_{sup} and T_{ret} and the logarithmic mean temperature difference $\Delta T_{ln} = \frac{T_{supply} - T_{return}}{\ln\left(\frac{T_{supply} - T_{room}}{T_{return} - T_{room}}\right)}$.
- Using the design heat flux in the heat flux equation

$$q = B\prod_i (a_i^{m_i})\Delta T_{ln} = K\Delta T_{ln} \quad (3)$$

we are able to determine the total heat transfer coefficient K. With K and mass flow determined, we finally calculate α using Equation (2).

We calculate K based on data available for the climate of Geneva. Values calculated with the above- described methodology vary slightly for the

two buildings as shown in Table 5.

When ordering space heating loads by ambient temperatures for selected building cases, separate clusters of space heating loads can be detected, mainly due to the influence of solar radiation and respective solar gains. In order to deduce unique heating curves, we filter the data to pick only values above the fourth quartile. With a bin size of 17 applied on the 8750 original data points, 980 and 1420 points remained for Building 1 and Building 2, respectively. Using the filtered data, we then estimate the heating curves, as shown in Fig. 9 together with the linear trends obtained.

Appendix C. Parametrization of SH system

The heat pump model required the definition of a nominal COP and nominal compressor power as sizing parameters. We defined the nominal COP as

$$COP_{nominal} = \eta \frac{T^{condenser}_{nominal}}{\left(T^{condenser}_{nominal} - T^{evaporator}_{nominal}\right)}, \tag{4}$$

where η is set to 0.5 and $T^{condenser}_{nominal}$ is given from the heating curve applied to the design temperature T^{air}_{design}, i.e. the lowest 1 % temperature of the selected climate (Geneva: −2.9 °C, Helsinki: −16.4 °C, Rome: 1.0 °C). Additionally, $T^{evaporator}_{nominal}$ reads

$$T^{evaporator}_{nominal} = T^{air}_{design} - \Delta T^{evaporator} - \Delta T^{hex}. \tag{5}$$

With the temperature difference at the evaporator $\Delta T^{evaporator} = 5$ K and the temperature difference across the heat exchanger $\Delta T^{hex} = 3$ K. Finally, the compressor power P^{comp} reads

$$P^{comp} = \frac{Q_{design}}{COP_{nominal}}. \tag{6}$$

Beside the parametrization of the heat pump model, we sized the SH buffer tank to mimic the thermal capacitance of the building, as the SH load is directly connected to the tank. Based on the assumptions that the typical required time to recharge the DHW tank Δt^{DHW} is three hours and that the SH buffer tank temperature T^{SH} was not allowed to decrease by more than 10 K during this period under maximum load (Q_{design}), the volume of the SH buffer tank then reads:

$$V^{SH} = \frac{Q_{design}\Delta t^{DHW}}{c_{p,w}\Delta T^{SH}}. \tag{7}$$

Appendix D. Closed-Loop configuration

See Fig. 10.

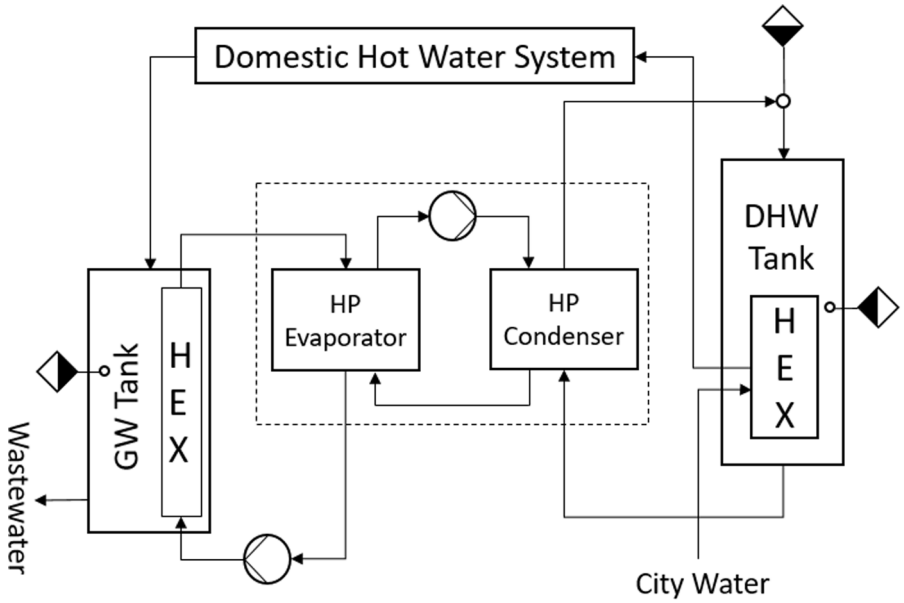

Fig. 10. Schematic diagram of the closed-loop configuration for the production of domestic hot water (DHW) using greywater (GW) as direct heat source for the heat pump (HP) evaporator. Contrary to the open-loop configuration – preheating ambient air – the unused heat at the evaporator is fed back into the system, hence the name "closed-loop".

References

[1] IEA. World Energy Balances 2017, ISBN: 9789264278097/9789264278103. 2017.
[2] Council EPa. Directive 2010/31/EU of the European Parliament and of the Council of 19 May 2010 on the energy performance of buildings, Official Journal of the European Union https://eur-lex.europa.eu/legal-content/EN/TXT/PDF/?uri=CELEX:32010L0031&from=EN (accessed 19.04.2021). 2010.
[3] Bundesamt für Energie. Gebäudepark 2050 - Vision des BFE. Bundesamt für Energie (ed) https://www.bfe.admin.ch/bfe/de/home/news-und-medien/publikationen.exturl.html/aHR0cHM6Ly9wdWJkYi5iZmUuYWRtaW4uY2gvZGUvcHVibGljYX/Rpb24vZG93bmxvYWQvODk4NQ==.html (accessed 19.04.2021). 2018.
[4] Bundesamt für Energie. Analyse des schweizerischen Energieverbrauchs 2000 - 2018 nach Verwendungszwecken, Prognos AG https://www.bfe.admin.ch/bfe/de/home/versorgung/statistik-und-geodaten/energiestatistiken/energieverbrauch-nach-verwendungszweck.exturl.html (accessed 19.04.2020). 2019.
[5] Fachvereinigung Wärmepumpen Schweiz (2019) Statistik 2019 https://www.fws.ch/wp-content/uploads/2020/04/FWS-Statistiken-2019_2.pdf (accessed 19.04.2021).
[6] Wellig B. Wärmepumpen-Forschung: Stand und künftige Herausforderungen. Proceedings of 25. Tagung des BFE-Forschungsprogramms «Wärmepumpen und Kälte» Burgdorf, 2019.
[7] Lazarova V, Choo K. and Cornel P. Water-energy interactions in water reuse, IWA Publishing, 2012, ISBN: 184339541X.
[8] Frijns J, Hofman J, Nederlof M. The potential of (waste)water as energy carrier. Energy Convers Manage 2013;65:357–63. https://doi.org/10.1016/j.enconman.2012.08.023.
[9] Müller, E.A., Schmid, F. and Kobel, B. (2009) Heizen und Kühlen mit Abwasser - Ratgeber für Bauträger und Kommunen. p. 36, Deutsche Bundesstiftung Umwelt https://www.waermepumpe.de/fileadmin/user_upload/waermepumpe/07_Publikationen/bwp-Heizen_und_Kuehlen_mit_Abwasser.pdf (accessed 07.07.2021).
[10] Wanner O, Panagiotidis V, Clavadetscher P, Siegrist H. Effect of heat recovery from raw wastewater on nitrification and nitrogen removal in activated sludge plants. Water Res 2005;39(19):4725–34. https://doi.org/10.1016/j.watres.2005.09.026.
[11] Hepbasli A, Biyik E, Ekren O, Gunerhan H, Araz M. A key review of wastewater source heat pump (WWSHP) systems. Energy Convers Manage 2014;88:700–22. https://doi.org/10.1016/j.enconman.2014.08.065.
[12] Shen C, Lei Z, Wang Y, Zhang C, Yao Y. A review on the current research and application of wastewater source heat pumps in China. Thermal Science and Engineering Progress 2018;6:140–56. https://doi.org/10.1016/j.tsep.2018.03.007.
[13] Nagpal H, Spriet J, Murali M, McNabola A. Heat Recovery from wastewater—A review of available resource. Water 2021;13(9):1274. https://doi.org/10.3390/w13091274.
[14] Golzar F, Silveira S. Impact of wastewater heat recovery in buildings on the performance of centralized energy recovery – A case study of Stockholm. Appl Energy 2021;297:117141. https://doi.org/10.1016/j.apenergy.2021.117141.
[15] Sitzenfrei R, Hillebrand S, Rauch W. Investigating the interactions of decentralized and centralized wastewater heat recovery systems. Water Sci Technol 2017;75(5–6):1243–50. https://doi.org/10.2166/wst.2016.598.
[16] Cooperman A, Dieckmann J, Brodrick J. Drain water heat recovery. ASHRAE Journal 2011;53:58–62.
[17] Gabor T, Dan V, Badila I-N, Tiuc A-E, Sur IM. Improving the energy efficiency of residential buildings by using a drain water heat recovery system. Environ Eng Manage J 2017;16(7):1631–6. https://doi.org/10.30638/eemj.2017.176.
[18] McNabola A, Shields K. Efficient drain water heat recovery in horizontal domestic shower drains. Energy Build 2013;59:44–9. https://doi.org/10.1016/j.enbuild.2012.12.026.
[19] Torras S, Oliet C, Rigola J, Oliva A. Drain water heat recovery storage-type unit for residential housing. Appl Therm Eng 2016;103:670–83. https://doi.org/10.1016/j.applthermaleng.2016.04.086.
[20] Zaloum C, Lafrance M. and Gusdorf J. Drain water heat recovery characterization and modeling. pp. 0-42 http://www.regie-energie.qc.ca/audiences/3637-07_2/DDR3637_2/RepDDR/B-12-GI-23Doc1-2_RepDDRSE-AQLPA_3637-2_28sept07.pdf (accessed 19.04.2021). 2007.
[21] Baek NC, Shin UC, Yoon JH. A study on the design and analysis of a heat pump heating system using wastewater as a heat source. Sol Energy 2005;78(3):427–40. https://doi.org/10.1016/j.solener.2004.07.009.
[22] Chen W, Liang S, Guo Y, Cheng K, Gui X, Tang D. Investigation on the thermal performance and optimization of a heat pump water heater assisted by shower waste water. Energy Build 2013;64:172–81. https://doi.org/10.1016/j.enbuild.2013.04.021.
[23] Dong J, Zhang Z, Yao Y, Jiang Y, Lei B. Experimental performance evaluation of a novel heat pump water heater assisted with shower drain water. Appl Energy 2015;154:842–50. https://doi.org/10.1016/j.apenergy.2015.05.044.
[24] Hervas-Blasco E, Pitarch M, Navarro-Peris E, Corberán JM. Optimal sizing of a heat pump booster for sanitary hot water production to maximize benefit for the substitution of gas boilers. Energy 2017;127:558–70. https://doi.org/10.1016/j.energy.2017.03.131.
[25] Meggers F, Leibundgut H. The potential of wastewater heat and exergy: Decentralized high-temperature recovery with a heat pump. Energy Build 2011;43(4):879–86. https://doi.org/10.1016/j.enbuild.2010.12.008.
[26] Ni L, Lau SK, Li H, Zhang T, Stansbury JS, Shi J, et al. Feasibility study of a localized residential grey water energy-recovery system. Appl Therm Eng 2012;39:53–62. https://doi.org/10.1016/j.applthermaleng.2012.01.031.
[27] Postrioti L, Baldinelli G, Bianchi F, Buitoni G, Maria FD, Asdrubali F. An experimental setup for the analysis of an energy recovery system from wastewater for heat pumps in civil buildings. Appl Therm Eng 2016;102:961–71. https://doi.org/10.1016/j.applthermaleng.2016.04.016.
[28] Seybold C, Brunk MF. In-house waste water heat recovery. REHVA Journal 2013:18–21.
[29] Hadengue B, Scheidegger A, Morgenroth E, Larsen TA. Modeling the water-energy nexus in households. Energy Build 2020;225:110262. https://doi.org/10.1016/j.enbuild.2020.110262.
[30] Elmqvist H. and Mattsson SE. Modelica — The next generation modeling language, an international design effort, pp. 1-5, Gent, Belgium. 1997.
[31] Wetter M, Zuo W, Nouidui TS, Pang X. Modelica Buildings library. J Build Perform Simul 2014;7(4):253–70. https://doi.org/10.1080/19401493.2013.765506.
[32] Hadengue B, Scheidegger A, Morgenroth E. and Larsen TA. The WaterHub Modules : material and energy flow analysis of domestic hot water systems. Proceedings of 13th International Modelica Conference, March 4-6, Regensburg, Germany, 2019, 639-646, DOI: 10.3384/ecp19157639.
[33] SVGW, Schweizerische Verein des Gas- und Wasserfaches (2020) W3/E3 d Richtlinie für Hygiene in Trinkwasserinstallationen https://www.svgw.ch/de/shopregelwerk/produkte/w3e3-d-richtlinie-fuer-hygiene-in-trinkwasserinstallationen/ (accessed 19.04.2021).
[34] Bundesamt für Statistik (2018) Bau- und Wohnungswesen 2016 https://www.bfs.admin.ch/bfsstatic/dam/assets/4966444/master (accessed 19.04.2021).
[35] Murray P, Marquant J, Niffeler M, Mavromatidis G, Orehounig K. Optimal transformation strategies for buildings, neighbourhoods and districts to reach CO2 emission reduction targets. Energy Build 2020;207:109569. https://doi.org/10.1016/j.enbuild.2019.109569.
[36] Crawley DB, Pedersen CO, Lawrie LK, Winkelmann FC. Energy plus: Energy simulation program. ASHRAE Journal 2000;42(4):49–56.
[37] Rhee K-N, Jeong C-H, Ryu S-R, Yeo M-S. and Seok H-T. A strategy to determine a heating curve for outdoor temperature reset control of a radiant floor heating system. Proceedings of Clima 2007 WellBeing Indoors, Helsinki (Finland), 2007.
[38] SVGW, Schweizerische Verein des Gas- und Wasserfaches (2015) Wasserverbrauch http://www.svgw.ch/fileadmin/resources/svgw/web/Wasser-Eau/SVGW_Wasserverbrauch_Haushalt_AeG_3_2015.pdf (accessed 19.04.2021).
[39] Ableitner L, Schöb S. and Tiefenbeck V. Digitalization of consumer Behavior – a descriptive analysis of energy use in the shower. Proceedings of INFORMATIK 2016 - Lecture Notes in Informatics (LNI), Bonn, 2016.
[40] Bertrand A, Aggoune R, Maréchal F. In-building waste water heat recovery: An urban-scale method for the characterisation of water streams and the assessment of energy savings and costs. Appl Energy 2017;192:110–25. https://doi.org/10.1016/j.apenergy.2017.01.096.
[41] Bertrand A, Mastrucci A, Schüler N, Aggoune R, Maréchal F. Characterisation of domestic hot water end-uses for integrated urban thermal energy assessment and optimisation. Appl Energy 2017;186:152–66. https://doi.org/10.1016/j.apenergy.2016.02.107.
[42] Butler D, Friedler E, Gatt K. Characterising the quantity and quality of domestic wastewater inflows. Water Sci Technol 1995;31:13–24.
[43] Friedler E, Butler D, Brown DM. Domestic WC usage patterns. Build Environ 1996;31(4):385–92.
[44] Pakula C, Stamminger R. Energy and water savings potential in automatic laundry washing processes. Energ Effi 2014;8(2):205–22. https://doi.org/10.1007/s12053-014-9288-0.
[45] Larsen TA, Hoffmann S, Luthi C, Truffer B, Maurer M. Emerging solutions to the water challenges of an urbanizing world. Science 2016;352(6288):928–33. https://doi.org/10.1126/science.aad8641.
[46] IEA, LowEx Communities - Optimised Performance of Energy Supply Systems with Exergy Principles (Annex 64) http://www.iea-ebc.org/Data/publications/EBC_Annex_64_Final_Report_September_2019.pdf (accessed 16.07.2021). 2019.
[47] DIN EN, Raumflächenintegrierte Heiz- und Kühlsysteme mit Wasserdurchströmung - Teil 2: Fußbodenheizung: Prüfverfahren für die Bestimmung der Wärmeleistung unter Benutzung von Berechnungsmethoden und experimentellen Methoden. 2013.